

# Diffuse Neutron Scattering Study of a Disordered Complex Perovskite $\text{Pb}(\text{Zn}_{1/3}\text{Nb}_{2/3})\text{O}_3$ Crystal

D. La-Orauttapong,<sup>1</sup> J. Toulouse,<sup>1</sup> J. L. Robertson,<sup>2</sup> and Z.-G. Ye<sup>3</sup>

<sup>1</sup>*Physics Department, Lehigh University, Bethlehem, PA 18015-3182*

<sup>2</sup>*Oak Ridge National Laboratory, Solid State Division, Oak Ridge, TN 37831-6393*

<sup>3</sup>*Department of Chemistry, Simon Fraser University, Burnaby, BC, V5A 1S6, Canada*

Diffuse scattering around the (110) reciprocal lattice point has been investigated by elastic neutron scattering in the paraelectric and the relaxor phases of the disordered complex perovskite crystal- $\text{Pb}(\text{Zn}_{1/3}\text{Nb}_{2/3})\text{O}_3$  (PZN). The appearance of a diffuse intensity peak indicates the formation of polar nanoregions at temperature  $T^*$ , approximately 40K above  $T_c=413\text{K}$ . The analysis of this diffuse scattering indicates that these regions are in the shape of ellipsoids, more extended in the  $\langle 111 \rangle$  direction than in the  $\langle 001 \rangle$  direction. The quantitative analysis provides an estimate of the correlation length,  $\xi$ , or size of the regions and shows that  $\xi_{\langle 111 \rangle} \sim 1.2\xi_{\langle 001 \rangle}$ , consistent with the primary or dominant displacement of Pb leading to the low temperature rhombohedral phase. Both the appearance of the polar regions at  $T^*$  and the structural transition at  $T_c$  are marked by kinks in the  $\xi_{\langle 111 \rangle}$  curve but not in the  $\xi_{\langle 001 \rangle}$  one, also indicating that the primary changes take place in a  $\langle 111 \rangle$  direction at both temperatures.

PACS Numbers: 77.84.Dy,61.12.Ld,77.80.-e

Many of the relaxor ferroelectrics known today are lead-based compounds with the perovskite structure. In addition to the characteristic frequency dispersion of their dielectric constant, several of them exhibit remarkable piezoelectric or electrostrictive properties that are finding important applications, e.g. as transducers and actuators. The  $\text{Pb}^{2+}$ -containing relaxor perovskites such as  $\text{Pb}(\text{R}_{1/3}\text{Nb}_{2/3})\text{O}_3$  ( $\text{R}=\text{Mg}^{2+}, \text{Zn}^{2+}$ ) have a common  $\text{ABO}_3$  cubic perovskite structure in which the B-site can be occupied by  $\frac{1}{3}\text{R}^{2+}$  and  $\frac{2}{3}\text{Nb}^{5+}$ . Because of the different atomic radii and valences of the B-site cation, PMN and PZN exhibit short-range chemical ordering [1,2]. Over the years, these relaxors and their properties have been described in a variety of ways, most often in terms of the formation of polar micro- or nanoregions [3,4]. However, these models are primarily based on indirect experimental evidence for such regions and more direct evidence is necessary in order to elucidate the true origin of the relaxor behavior. For this purpose, neutron and X-ray techniques are most suitable, as they can provide evidence of local structural ordering. Obtaining such evidence is crucial if the formation of polar regions is indeed responsible for the relaxor behavior.

PZN is a prototype relaxor ferroelectric. It was found to exhibit a large dielectric dispersion and a broad dielectric maximum that depended on both frequency and temperature. Earlier studies also reported a phase transition near 413K [5,6], which fell in the temperature region of the maximum of the dielectric peak. More recent studies only mention the coexistence of cubic and rhombohedral phases, with polar nanodomains growing into polar microdomains [7] and their volume fraction increasing with decreasing temperature. Strain appears to play an important role in a nanodomain-to-microdomain phase transition, which therefore resembles a martensitic phase transformation [7]. In the last few years, PZN has also

been intensively investigated in the form of a solid solution with  $\text{PbTiO}_3$  [8–10], because of its enhanced dielectric and piezoelectric properties. PZN is already a disordered perovskite in the cubic phase [11], with individual Pb atoms shifted from the A-site position along one of eight equivalent  $\langle 111 \rangle$  directions and O atoms forming a ring-like distribution within  $\{100\}$  planes. In contrast, the Zn/Nb atoms remain located at the normal B-site position. In the rhombohedral phase, the displacements of Pb and O atoms become correlated, both along a specific  $[111]$  direction, with  $\delta r_{\text{Pb}} = 0.31 \text{ \AA}$  and  $\delta r_{\text{O}} = 0.17 \text{ \AA}$  at 295K. More specifically, a recent X-ray study [12] of the related system PMN suggests that the three oxygen atoms may be displaced along three converging  $[110]$  directions, all three pointing towards the same A position, such that the average oxygen displacement or the net oxygen dipole moment in the unit cell is indeed along the same  $[111]$  direction as that of Pb. It is important to note that the displacement of Pb [11] as well as its neutron scattering length are almost twice those of the O atom.

In the present paper, we report the results of a diffuse neutron scattering study of PZN, in order to identify and directly monitor the formation of polar nanoregions resulting from the correlated displacements of the Pb and O atoms. This study follows a similar study of another mixed perovskite relaxor,  $\text{K}_{1-x}\text{Li}_x\text{TaO}_3$  (KLT), which provided the correlation length or size of the polar nanoregions as a function of temperature [13]. In contrast to KLT, PZN exhibits not only substitutional chemical disorder but also charge disorder. Moreover, due to the lone electron pair effects,  $\text{Pb}^{2+}$  ions form partially covalent bonds with the neighboring oxygen atoms, which results in the off-centering of lead and in an additional local electric dipole moment [14]. Our purpose here is to provide direct evidence for these regions and

to characterize them in a single crystal of PZN.

In complex perovskites such as PZN, the diffuse scattering has two possible origins [15]: i) different scattering factors of the two possible atoms ( $B_1, B_2$ ) occupying a given B site ( $j$ ), or ii) static displacements away from this site. Both factors arise from concentration inhomogeneities in the compound and may simultaneously contribute to the diffuse scattering. It is well known that the static structure factor is given by [16]:

$$F(\mathbf{Q}) = \sum_j b_j e^{i\mathbf{Q}\cdot\mathbf{r}_j} e^{-W_j} \quad (1)$$

where  $b_j$  is the neutron scattering length,  $e^{-W_j}$  is the Debye-Waller factor for the  $j$ th atom with coordinate  $\mathbf{r}_j$  in the unit cell and the summation is carried out over all positions occupied in the unit cell. The scattering vector  $\mathbf{Q}$  is defined as  $\mathbf{k} - \mathbf{k}'$ . In the presence case, small displacements,  $\delta\mathbf{r}$ , of the atoms from their normal positions distort the local cubic symmetry such that  $\mathbf{r}_j = (\mathbf{r} + \delta\mathbf{r})_j$ . At high temperature, these displacements vary both in magnitude and direction. The scattered intensity is proportional to  $F^2 = F.F^*$  so that, experimentally, it is possible to determine the amplitude  $F$  of the structure factor but not its phase. For the sake of argument we omit the Debye-Waller factor in the following calculation. In accordance with Ref. [11], which reported the Zn/Nb atoms at their ideal perovskite position at all temperatures, no displacement is included in eq. (1) for the atoms at the B-site. With the origin chosen at the Pb site, eq. (1) and for small displacements of the Pb and O atoms, the neutron scattering structure factor  $F$  can then be evaluated at the (110) reciprocal lattice point:

$$F(\mathbf{Q}) = \underbrace{[b_{\text{Pb}} + b_{\text{Zn/Nb}} - b_{\text{O}}]}_{\text{Bragg}} + \underbrace{i\mathbf{Q}\cdot[\delta\mathbf{r}_{\text{Pb}}b_{\text{Pb}} + (\delta\mathbf{r}_{\text{O1}} - \delta\mathbf{r}_{\text{O2}} - \delta\mathbf{r}_{\text{O3}})b_{\text{O}}]}_{\text{Diffuse}} \quad (2)$$

where  $b_{\text{Pb}}$ ,  $b_{\text{Zn/Nb}}$ , and  $b_{\text{O}}$  are the scattering lengths of Pb, Zn/Nb, and O atoms respectively. The scattering lengths for the Zn/Nb atoms can be found from  $b_{\text{Zn/Nb}} = \frac{1}{3}b_{\text{Zn}} + \frac{2}{3}b_{\text{Nb}}$ . In the structure factor above, we have separated the Bragg scattering contribution which contains information about the average lattice from the diffuse scattering which arises from local deviations from the ideal structure. These deviations result from correlated displacements of atoms. In the presence case, the diffuse scattering is primarily associated with the Pb atom, which is strongly off-centered in the  $\text{PbO}_{12}$  unit and has almost twice the neutron scattering length of the O atom. In addition, because of the Pb displacement along the [111] direction,  $\delta r_{\text{Pb}}$  is expected to make a greater contribution in that direction than along the [001] and [110] directions.

The neutron scattering experiments were performed on the HB-1 triple-axis spectrometer of the High Flux Isotope Reactor at Oak Ridge National Laboratory. Pyrolytic graphite (002) crystals were used for both the monochromator and analyzer, to suppress harmonic contamination. The collimation was 48'-20'-20'-70' and the incident neutron energy was 13.6 meV ( $\lambda=2.453\text{\AA}$ ). Initially, the scattering around the (110) reciprocal lattice point in the ( $hhl$ ) plane was studied because the (110) reflection has the largest structure factor [1]. In each scan, the stepsize was  $\delta q = 0.01$  reciprocal lattice units (rlu) or  $0.016 \text{ \AA}^{-1}$ . The yellowish single crystal of  $\text{Pb}(\text{Zn}_{1/3}\text{Nb}_{2/3})\text{O}_3$  used in the experiment was grown by a high temperature solution growth technique [17]. The measurements were performed at temperatures from 350 K to 550 K.

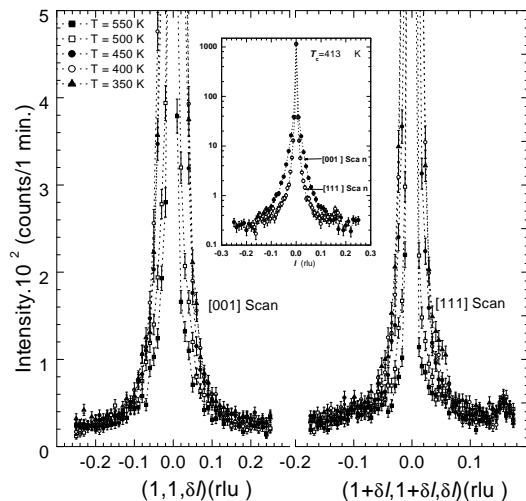


FIG. 1. Elastic diffuse scattering of neutrons in the [001] and [111] directions near the (110) reciprocal lattice point at  $T=550, 500, 450, 400,$  and  $350\text{K}$ . Inset is scattering intensities at  $T_c=413\text{K}$  in the [001] and [111] directions.

The narrow Bragg peak as well as the relatively broad diffuse scattering peak at the (110) reciprocal lattice point are presented in Fig.1 for several temperatures. As expected, the Bragg scattering is equally strong in both the [001] and [111] scans (inset of Fig.1). However, the diffuse scattering is more extended in the [001] than in the [111] direction, having the form of a rod along a cubic direction. It is important to note that the diffuse scattering is more extended in a direction in which the correlation length  $\xi$  is shorter. We will discuss this point later. In order to separate the Bragg and diffuse scattering contributions, the intensity,  $I(q)$ , was fitted as the sum of a Gaussian and a Lorentzian, using a least-squares method (Fig.2). In the inset of Fig.2, the Bragg intensity is seen to increase slowly, starting at approximately 500K, then more rapidly below 400K. The latter rapid increase of the Bragg intensity can be explained by i) a relief of extinction due to an increase in mosaic-

ity below the transition or ii) an unusual behavior of the Debye-Waller factor due to freezing of certain atomic motion at lower temperatures. A broadening of the Bragg peak is normally observed to accompany the freezing process but is not observed here. This would rule out the effect of the Debye-Waller factor in the present case and favor the first explanation. In fact, a similar behavior was observed in a single crystal of PMN by Gosula et al. [18] using X-ray diffuse scattering. They speculated that the sharp increase in intensity arose from the anti-ferrodistortive ordering that developed at low temperatures. This anti-ferrodistortive ordering grows to a

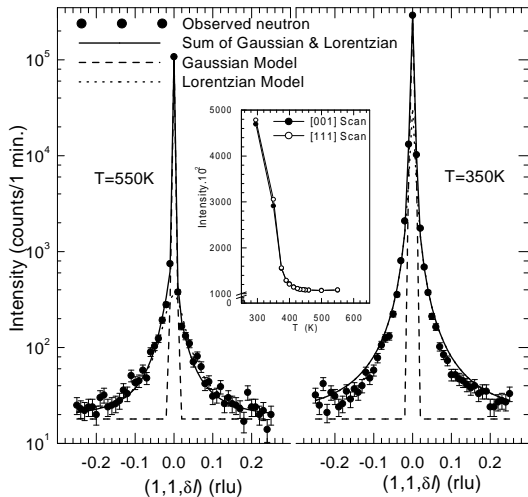


FIG. 2. Elastic neutron scattering in the [001] direction at  $T=550$  and  $350\text{K}$ . The solid curve shows the scattering profile fitted by the sum of a Gaussian and a Lorentzian and the two components (dash and dot curves) are shown separately. Inset is temperature dependence of Bragg peak intensities in the [001] and [111] directions.

Turning to the diffuse scattering component, in Fig. 2, the  $q$  or  $l$ -dependence of the scattered intensity is presented on a semilogarithmic plot at  $550\text{K}$  and  $350\text{K}$ . The Lorentzian function used in the fit of the experimental  $I(q)$  curves, yielded a peak intensity and a full width at half-maximum ( $\Delta q_{FWHM}$ ). Such a Lorentzian line-shape is predicted by the Ornstein-Zernike model [19]:  $I \simeq \frac{1}{q^2 + \xi^{-2}}$  where  $q$  is the scattering vector defined as  $\mathbf{q} = \mathbf{k} - \mathbf{k}'$  and  $\xi$  is the correlation length. The Ornstein-Zernike model assumes a correlation function of the form  $\frac{e^{-\frac{r}{\xi}}}{r}$  for the polarization. Therefore the diffuse scattering width at half maximum,  $\Delta q_{FWHM}$ , provides an estimate of  $\xi$  or, equivalently, of the size of the polar nanoregions:  $\xi = \frac{a}{\pi \Delta q_{FWHM}}$  where  $a$  is the lattice parameter. The Lorentzian fit parameters,  $I(q)_{\max}$ ,  $\Delta q_{FWHM}^2$ , and  $\xi$ , are shown in Fig. 3 (a) and (b) as a function of temperature. In both the [001], and [111] directions, the results indicate that:

i) the diffuse scattering peak intensity,  $I(q)_{\max}$ , increases as the temperature decreases. It is interesting however to note that the peak intensity, as measured in the [111] direction, goes through a plateau around the transition temperature ( $T_c = 413\text{K}$ ) before increasing again below  $400\text{K}$ . This feature is much less visible in the [001] direction, for which the intensity increases continuously. Fig. 3 (a) also shows that the strongest diffuse scattering is observed in the [111] direction, an observation that is consistent with the displacement of the Pb atoms producing the local polarization in the rhombohedral phase. The diffuse scattering intensity is in fact generally proportional to  $\langle P_{local}^2 \rangle$  [20]. Consequently, an increase of the diffuse scattering intensity with decreasing temperature reflects the growth of the polar clusters or the net correlated displacements of lead and oxygen atoms in a [111] direction as reported in Ref. [11] for PZN. It is also in agreement with the structure factor calculation  $F$  developed above, which predicts a greater magnitude of  $F \cdot F^*$  along the [111] direction than along th

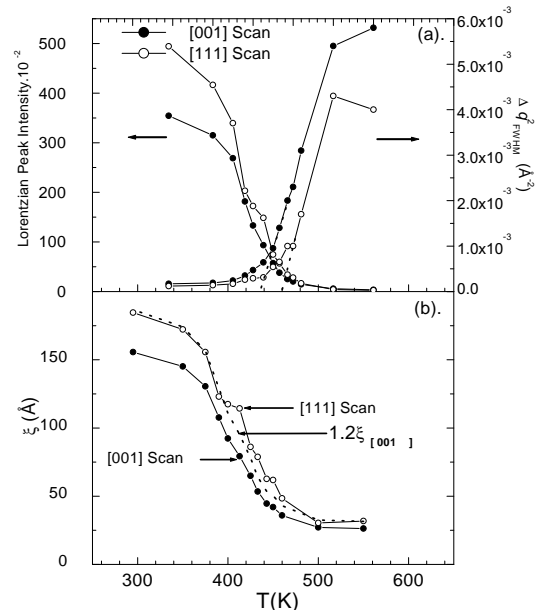


FIG. 3. Temperature dependence of (a) the Lorentzian Peak Intensity and square of the FWHM,  $\Delta q_{FWHM}^2$ , (b) the correlation length,  $\xi$  in the [001] and [111] directions.

ii) the width squared,  $\Delta q_{FWHM}^2$ , initially decreases almost linearly with temperature, but then deviates from a straight line at approximately  $450\text{K}$ , or  $40$  degrees above the transition ( $T_c = 413\text{K}$ ) and subsequently levels off at low temperature. The initial linear dependence is the manifestation of a Curie-Weiss law. This should be expected in a temperature range in which the polarization fluctuations are dynamic, since the correlation length squared,  $\xi^2$ , is proportional to the dielectric constant,  $\epsilon$ , [21] which itself is expected to follow a Curie-Weiss law initially:

$$\frac{1}{\Delta q_{FWHM}^2} \sim \epsilon = \frac{C}{T - T_c} \quad (3)$$

where  $C$  is the Curie constant. The departure of  $\Delta q_{FWHM}^2$  from a linear dependence, seen in Fig.3 (a), marks the appearance of long-lived polar fluctuations or permanent polar regions in the crystal, accompanied by local strain fields. This also explains the simultaneous increase in Bragg intensity noted above, due to an increase in mosaicity. It is worth noting that a very similar evolution has been reported by Iwase et al. [11] for the lattice constant, but with a departure from a linear dependence at approximately 550K instead of 450K. However, their measurements were made on a powder obtained from a ground crystal and it is well known that relaxors are very susceptible to internal strains.

iii) the correlation length,  $\xi$ , shown in Fig.3 (b) increases continuously with decreasing temperature and saturates at low temperatures. This is uncommon for conventional ferroelectrics, in which the correlation length decreases below the transition. The present behavior indicates that the low temperature state is not a homogeneous ferroelectric state but, rather, a mesoscopic one, presumably made of large polar regions. At  $T_c = 413\text{K}$ , the finite size of the polar regions is  $\sim 79\text{\AA}$  (19 unit cells) and  $\sim 114\text{\AA}$  (28 unit cells) respectively in the [001] and [111] directions. The longer correlation length or effective size of the polar regions in the [111] direction is found to be  $\xi_{[111]} \sim 1.2\xi_{[001]}$  (see dotted line in Fig.3b), consistent with the larger Pb displacement component in the [111] direction. This result suggests that the polar regions are in the form of ellipsoids, preferentially oriented in [111] directions. Another noticeable difference between the two directions is the appearance of two kinks in the  $\xi_{[111]}$  curve, at  $\sim 450\text{K}$  and  $\sim 413\text{K}$ , that are not visible in the  $\xi_{[001]}$  curve. As discussed above, the first one, at 450K, reveals the relatively sudden formation of permanent polar regions, and the second one corresponds to the transition at  $T_c$ . The absence of these kinks in the  $\xi_{[001]}$  curve indicates that the growth of the correlation length in that direction is only indirectly affected by the formation of the polar regions at 450K and by their collective realignment at the transition at 413K. This result is also consistent with the primary net displacements of Pb and three O atoms in one of eight possible [111] directions.

In conclusion, thermal diffuse neutron scattering measurements in the paraelectric and relaxor temperature regions of the PZN crystal clearly reveal the relatively abrupt formation of polar nanoregions at 450K, approximately 40 degrees above the transition at  $T_c = 413\text{K}$ . With decreasing temperature, these polar regions grow and so does their volume fraction. The correlation lengths in the two directions studied are found to be in the ratio  $\xi_{[111]} \sim 1.2\xi_{[001]}$  over the whole temperature range, except for two kinks in the  $\xi_{[111]}$  curve at 450K

and 413K. The fact that the correlation lengths remain high below the transition indicates that, at low temperature, the polar regions subsist at low temperature in what can be called a mesoscopic ferroelectric phase. Diffuse scattering results at other reciprocal lattice points are presently being analyzed and will be reported in a subsequent paper.

We wish to thank R.K. Pattnaik and G. Shirane for helpful discussions. This work was supported by DOE Grant No. DE-FG02-00ER45842 and ONR Grant No N00014-99-1-0738 as well as the Oak Ridge National Laboratory at the High Flux Isotope Reactor.

- 
- [1] Y.Yokomizo, T. Takahashi, and S. Nomura, J. Phys. Soc. Jpn. **28**, 1278 (1970).
  - [2] C.A. Randall and A.S. Bhalla, Jpn. J. Appl. Phys. **29**, 327 (1990).
  - [3] G.A. Smolensky, J. Phys. Soc. Jpn. **28**, Suppl. 26 (1970).
  - [4] L.E. Cross, Ferroelectrics **76**, 241 (1987).
  - [5] N.P. Khuchua, V.A. Bokov, and I.E. Myl'nikova, Sov. Phys.-Solid State. **10**, 194 (1968).
  - [6] J. Kuwata, K. Uchino, and S. Nomura, Ferroelectrics **22**, 863 (1979).
  - [7] M. Mulvihill, L.E. Cross, W. Cao, and K. Uchino, J. Am. Ceram. Soc. **80**, 1462 (1997).
  - [8] J. Kuwata, K. Uchino, and S. Nomura, Jpn. J. Appl. Phys., Part1 **21**, 1298 (1982).
  - [9] S-F. Liu, S-E. Park, T.R. Shrout, and L.E. Cross, J. Appl. Phys. **85**, 2810 (1999).
  - [10] P.M. Gehring, S.-E. Park, and G. Shirane, Phys. Rev. Lett. **84**, 5216 (2000).
  - [11] T. Iwase, H. Tazawa, K. Fujishiro, Y. Uesu, and Y. Yamada, J. Phys. Chem. Solids. **60**, 1419 (1999).
  - [12] N. Takesue, Y. Fujii, and H. You, (unpublished).
  - [13] G. Yong, J. Toulouse, R. Erwin, S. Shapiro, and B. Hennen, Phys. Rev. B **62**, 14736 (2000).
  - [14] T. Egami, S. Teslic, W. Dmowski, P.K. Davies, and I.-W. Chen, J. Korean Phys. Soc. **32**, S935 (1998).
  - [15] M.A. Krivoglaz, Theory of X-Ray and Thermal-Neutron Scattering by Real Crystals, Plenum Press, New York (1969).
  - [16] W. Schmatz, in X-ray and Neutron Scattering Studies on Disordered Crystals (Edited by Herbert Herman), p.105, New York and London (1973).
  - [17] L. Zhang, M. Dong and Z.-G. Ye, Mater. Sci. Eng. B. **78**, 96 (2000).
  - [18] V. Gosula, A. Tkachuk, K. Chung, and H. Chen, J. Phys. Chem. Solids. **61**, 221 (2000).
  - [19] H.E. Stanley, Introduction to Phase Transitions and Critical Phenomena, Oxford University Press, (1971).
  - [20] K. Nomura, T. Shingai, S. Ishino, H. Terauchi, N. Yasuda, and H. Ohwa, J. Phys. Soc. Jpn. **68**, 39 (1999).
  - [21] F. Jona. and G. Shirane, Ferroelectric Crystals, Dover Publications, New York (1962).